

A simple correlation between texture and earing

M Benke¹, A Hlavacs¹, D Petho¹, D A Angel¹, M Sepsi¹, E Nagy², V Mertinger¹

¹ University of Miskolc, Institute of Physical Metallurgy, Metalforming and Nanotechnology, Miskolc-Egyetemváros, Hungary

² MTA-ME Materials Research Group, Miskolc-Egyetemváros, Hungary

E-mail: fembenke@uni-miskolc.hu

Abstract. The phenomenon of earing has been known since the rise of deep drawing process. It has been early recognized, that earing is caused by the plastic anisotropy of textured materials. Over the past decades, there have been many methods proposed to find a way to predict earing through either mechanical tests, the combination of texture data evaluation and strain calculations, or finite element analysis. The objective of the present study is to propose a simple, yet suitable method, with which the average earing value of a blank can be estimated. The method solely requires measured texture (ODF) data and is based on defining every individual texture component pole as the vectorial combination of their (+) and (-) earing direction components. The method was tested on a sample series with different average earing values taken from an industrial rolled and annealed, 3003 type Al semi-product coil. Satisfactory correlation was found between estimated and measured earing numbers.

1. Introduction

During deep drawing of a cylindrical cup, different height forms along the circumference if the blank is anisotropic. The phenomenon is called earing and is caused by the plastic anisotropy of textured polycrystalline sheets. The demand to connect the observed earing to texture exists since the 1940s. Over decades, there have been quite many attempts to find the correlation between earing and texture. Fukui and Kudo [1], later Grewen [2] found that earing is predictable from the Lankford number (Δr). Tucker's method [3] was based on single slip and Schmid's law and was able to predict earing of a single crystalline material. His concept was applied to polycrystalline cases by Kanetake et al. [4], where tensile radial stress, compressive tangential stress and zero normal stress (to blank surface) was assumed during deep drawing and the bulk material was simplified to be an agglomerate of individual single crystals with certain orientations whose volume fractions were obtained from the orientation distribution function (ODF). Using empirical values in the work-hardening rule of crystals on earing, they accurately calculated not only the positions, but also the height of peaks within a blank. The model proposed by Da Costa Viana et al. [5] was based on combining ODF data with yield locus calculation. They assumed that the radial strains within sheets are inversely proportional to yield stresses. The method was able to predict the shape of earing, but it was not clarified whether their method predicted ear height. Pochinotto et al. [6] proposed a more sophisticated calculation, in which stress equilibrium equations were used. They obtained very good correlation between predicted and measured earing. Rodrugues and Bate [7] improved the previous concept, but their solution was suitable only for the four-ear cases. Moreover, they assumed that during deep drawing, tangential stress is compressive, normal stress is zero and radial stress is also zero, which is only valid for the outside edge of the blank. This was refined by Van Houtte [8]. All the above described methods predict the locations of peaks and troughs within a deep draw print



through additional mechanical tests, or evaluating the ODF and calculating the strain field or yield locus. Recently, earing is usually analyzed through finite element (FE) simulations. For those, the function describing the material's plastic anisotropy, which is implemented as user subroutines, is in the focus during development [9-11].

The aim of the present manuscript is to present a simple, yet suitable method to estimate earing directly and solely from the texture measurement (ODF) data. At first, only the value of average earing of a blank is dealt with.

2. Experimental

2.1. Sampling

The examined samples were taken from an industrial size, 3003 type aluminum coil manufactured by ARCONIC-Köfém Ltd. where the main production steps include closed direct chill casting, homogenization, hot-rolling, cold-rolling, annealing and finishing operations. In the annealed state, full-width sections were cut from the front and middle (along the length) of the coil. Samples were taken from five locations across the cross sections, namely: center, (C) side 1 quarter (Q1), side 1 edge (E1), side 2 quarter (Q2), side 2 edge (E2) for XRD and deep draw tests, according to Fig. 1. In the figure, it can also be seen that the XRD and deep draw test samples were taken out from as close as possible.

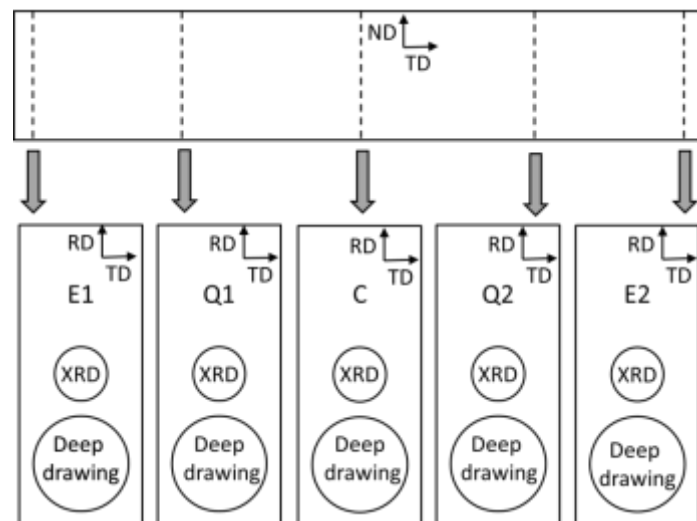


Figure 1. Sampling locations for XRD texture and deep drawing tests along the cross sections of the industrial coil. The reference rolling coordinate system is also marked.

2.2. Texture measurements

X-Ray diffraction measurements were performed with a Bruker D8 Advance type diffractometer equipped with an Eulerian cradle and CoK α tube (40 kV, 40 mA). The partial (0° - 75°) $\{111\}$, $\{200\}$ and $\{220\}$ pole figures were measured and corrected for defocusing. After recalculation, the ODFs were obtained using the harmonic method with TexEval software. The main texture components were calculated with 10° scatter.

2.3. Determination of earing

It is commonly observed, that after cold rolling, the ears appear in the $45^\circ(+n \cdot 90^\circ)$ directions relative to rolling direction (RD), while after annealing in the RD and transverse direction (TD) ($+n \cdot 90^\circ$) directions (Fig. 2.a). (Cold rolling earing is often called “-” earing, while annealed is called “+” earing. However, the signs are only labels, they have no mathematical sense.)

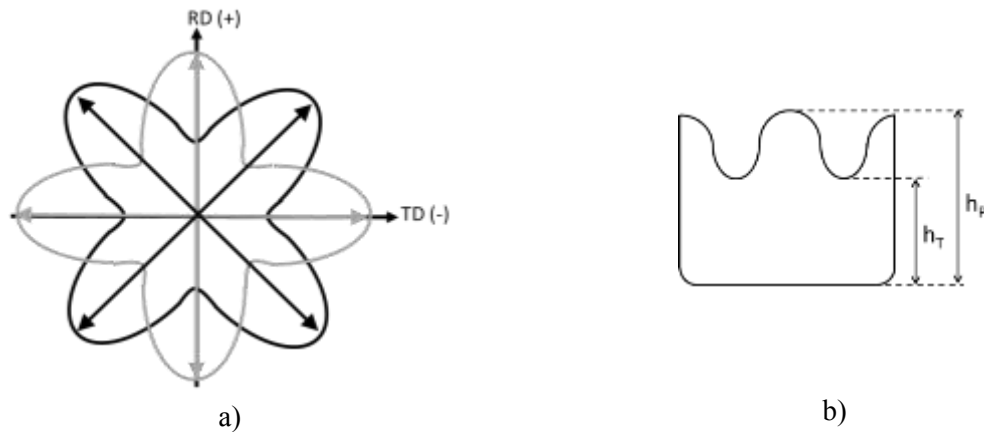


Figure 2. a) Peak and valley heights in case of earing, b) earing directions after cold rolling (black) and annealing (grey).

In general, earing is characterized by deep-draw tests, which, in this case, were carried out by ARCONIC-Köfém Ltd. After deep drawing, the average height of the peaks (h_p^{AV}) and troughs (h_T^{AV}) were measured according to (1) and (2), respectively (Fig. 2. b).

$$h_p^{AV} = \frac{\sum_{i=1}^n h_{p_i}}{n_p} \quad (1)$$

$$h_T^{AV} = \frac{\sum_{i=1}^n h_{T_i}}{n_p} \quad (2)$$

Afterwards, the difference (h_D) between average peak height (h_p^{AV}) and troughs (h_T^{AV}) was calculated according to (3), and the mean height (h^{AV}) was calculated by (4).

$$h_D = h_p^{AV} - h_T^{AV} \quad (3)$$

$$h^{AV} = \frac{h_p^{AV} + h_T^{AV}}{2} \quad (4)$$

Finally, earing (Z) was calculated according to (5).

$$Z = \frac{h_D}{h^{AV}} * 100 \quad (5)$$

2.4. Calculation of the Vectorial Earing Ratio

In Fig. 3, poles of the main texture components (C, S, B, Cube, G) [12, 13] are presented on the $\{h00\}$ pole figure. It can be clearly seen, that in the recrystallized state, the Cube and G components can be found along the RD and TD ($+n*90^\circ$) directions. Comparing to Fig. 2. these are the directions, where the ears (peaks) appear after annealing. On the other hand, poles of the C, S and B components can be found close to the 45° ($+n*90^\circ$) directions relative to RD. Again, these are the directions, where the ears appear after cold rolling (Fig. 2.). This purely empirical observation had already been recognized by many experts previously [8, 14-19]. Hence, the correlation between $\{h00\}$ poles of the main texture components and the macroscopic formability is recognized.

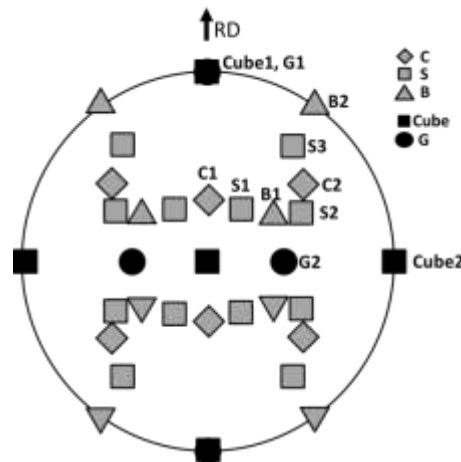


Figure 3. Poles of the main texture components (C, S, B, Cube, G) on the {200} pole figure [20].

This correlation can be more precisely described if it is examined, what is the contribution of an individual texture component pole P to the “+” and “-” earing. This is shown in Fig. 4, as follows. The direction of “+” earing overlaps with the RD and TD, while the direction of “-” earing is marked with the line 45° relative to RD. The location vector L (pointing to P from the origin O) can be resolved as the sum of vectors $OD+DP$, where OD is the contribution of P to (-) earing, and DP to (+) earing. If the pole coordinates, α (the altitude angle of P) and β (the azimuth angle of P) are known, OD and DP can be calculated. Due to the stereographic projection, the length of L linearly increases with α and reaches 1 if $\alpha=90^\circ$. Thus, L can be calculated according to (6).

$$L = \frac{\alpha}{90} \quad (6)$$

The projection of L to TD ($Proj_{TD}$) can be calculated within the triangle OPT as follows:

$$Proj_{TD} = |L| \cos(90 - \beta) \quad (7)$$

Similarly, the projection of L to RD ($Proj_{RD}$) can be obtained from the triangle OPR:

$$Proj_{RD} = |L| \cos \beta \quad (8)$$

If the pole P is located between RD and (-) (Fig. 4 a.), OD can be obtained within the ODT triangle as:

$$OD = \frac{Proj_{TD}}{\cos 45^\circ} \quad (9)$$

Afterwards, the projection of OD to RD (r) within the ODR' triangle is:

$$r = OD * \sin 45^\circ \quad (10)$$

Finally, DP can be achieved by (11):

$$DP = Proj_{RD} - r \quad (11)$$

If the pole P is located between (-) and TD (Fig. 4 b.), OD is as determined from the triangle ODR as follows:

$$OD = \frac{Proj_{RD}}{\cos 45^\circ} \quad (12)$$

Hence, the projection of OD to TD (t) within the ODT' triangle is:

$$t = OD * \cos 45^\circ \quad (13)$$

At the end, DP can be written as:

$$DP = Proj_{TD} - t \quad (14)$$

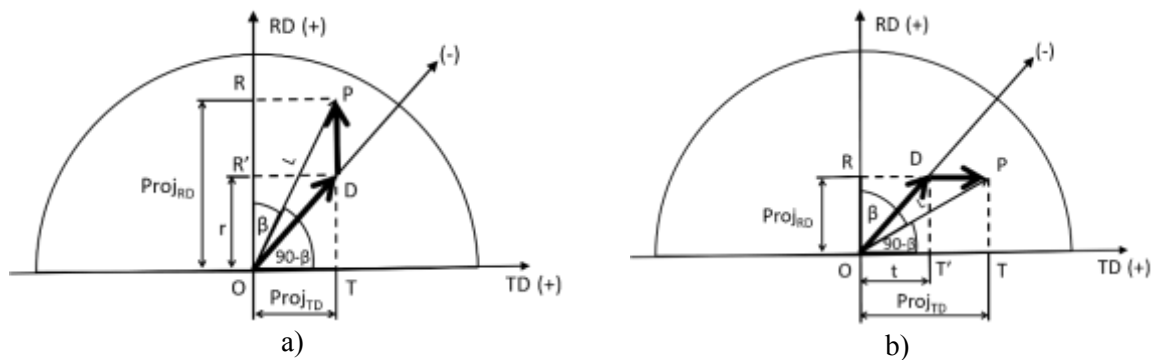


Figure 4. The (+) and (-) vectoral components of an individual pole P. a) P is between RD and (-) b) P is between (-) and TD

In Fig. 3, it was seen that one texture component has multiple poles on the $\beta=0^\circ-90^\circ$ quarter pole figure (namely, C1, C2, S1, S2, S3, B1, B2, Cube1, Cube2, G1, G2). The (+) and (-) vectoral components ($COMP_{i,j}^+ \equiv DP$ and $COMP_{i,j}^- \equiv OD$, respectively) of all main texture component poles were calculated and multiplied with the volume fractions of the texture components (V_i). This previous calculation was performed only within the $\beta=0^\circ-90^\circ$ quarter pole figure. However, since the calculation of earing is based on the average of all peak heights and not only the maximal peak height of the ears, the full pole figure (the $\beta=0^\circ-360^\circ$) must be considered. Therefore, the vectoral components were multiplied with the total number of the poles ($n_{i,j}$) (15) and (16) to obtain the vectoral sum of all texture component poles in the (+) and (-) directions (V_+ and V_- , respectively). Finally, the larger one of V_+ and V_- was divided with the smaller one (17) to get the Vectoral Earing Ratio (VER).

$$V_+ = \sum_{i=1}^n n_{i,j} (V_i * COMP_{i,j}^+) \quad (15)$$

$$V_- = \sum_{i=1}^n n_{i,j} (V_i * COMP_{i,j}^-) \quad (16)$$

$$VER = \frac{MAX(V_+, V_-)}{MIN(V_+, V_-)} \quad (17)$$

3. Results

Figure 5. shows the variation of measured (+) type earing together with the calculated texture component volume fractions across the front cross section (a) and the middle cross section (b) of the examined coil. It is apparent that earing strongly varies across both sample series. It is high at the edges (~5-6%), while low in the center regions (~1-2%). The texture component volume fractions also show significant

deviations. The strongest texture component is the Cube, which, similarly to earing, is highest at the edges. However, no straight correlation can be seen between either texture component volume fraction and earing.

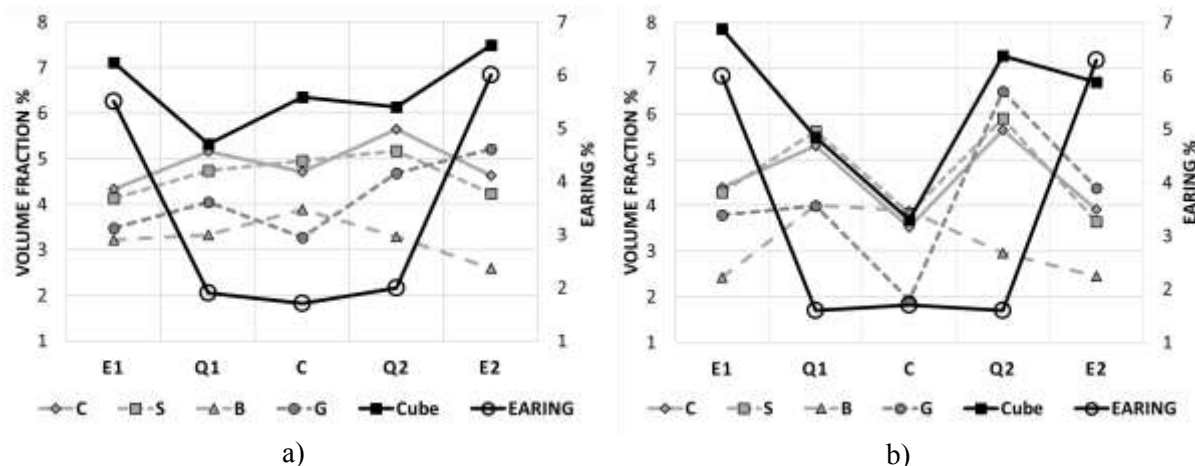


Figure 5. Variation of measured (+) type earing and texture component volume fractions a) across the front cross section b) across the middle cross section.

Figure 6. shows the measured (+) type earing and the calculated Vectorial Earing Ratio variation across the front (a) and middle (b) cross sections. In the sample series taken from the front cross section, the tendency of Vectorial Earing Ratio has a good correlation with that of the measured earing. In case of series from the middle cross section, the two variations are in a good agreement, except the sample Q2, where Vectorial Earing Ratio is somewhat high compared to the measured earing. However, this slight deviation can originate from the fact that the samples for deep drawing and XRD examinations were not taken from the same exact location, and, as seen, the texture of the sample series shows a quite strong texture inhomogeneity along the coil length and across the cross section.

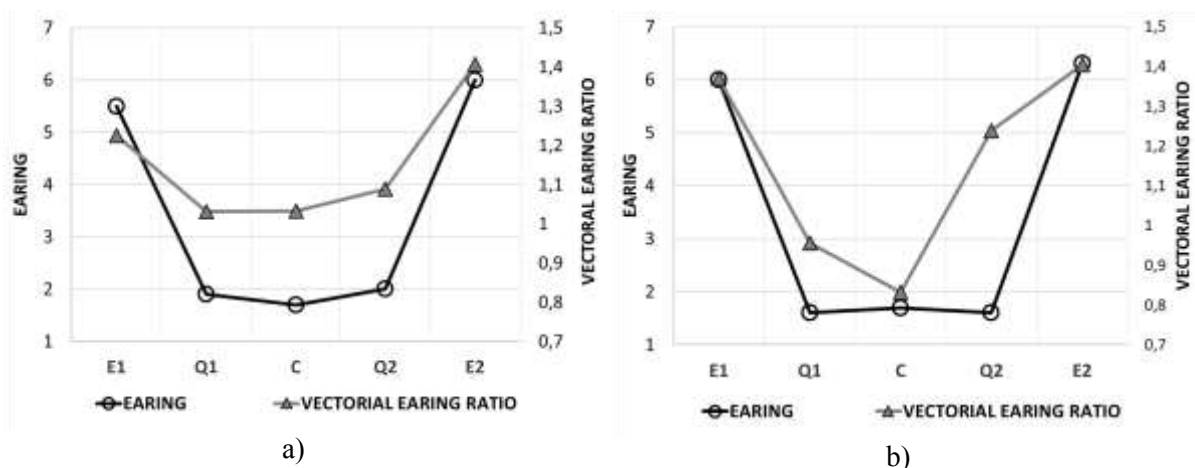


Figure 6. Variation of measured (+) type earing and calculated Vectorial Earing Ratios a) across the front cross section b) across the middle cross section.

4. Conclusions

It was seen that the main texture component volume fractions, as single quantities, did not exhibit a straightforward correlation with the measured earing across the cross sections of 3003 type aluminum sheet being in rolled+annealed state. This is understandable, since all texture components have an effect (smaller or larger) on formability, thus, the observed earing is governed by the combination of all texture

components that are present. A method was presented in this manuscript which proposes a geometrical connection between the texture components and the magnitude of earing (both (+) and (-) type). The proposed calculation is based on defining all texture component poles as the vectorial combination of their (+) and (-) earing direction components. The method supposes that unless the pole is located exactly on the (+) or (-) directions, it has a contribution to both (+) and (-) type earing. It follows that from the calculation point of view, the method does not differentiate between rolling and recrystallization texture components. The calculated Vectorial Earing Ratio is the ratio of the sum of (+) and (-) earing contribution of all poles considered. The obtained results show that a good correlation was achieved between the calculated Vectorial Earing Ratio and earing.

Acknowledgments

The described research work was supported through the National Research, Development and Innovation Office – NKFIH K119566 project.

References

- [1] Fukui S and Kudo H 1950 *Rep. Inst. Sci. Tech. Univ. Tokyo* **4** p 33
- [2] Grewen J 1971 *Quantitative Analysis of Textures Proc. Int. Seminar (Cracow)* p 195
- [3] Tucker G E G 1961 *Acta Metall.* **9** 275-286
- [4] Kanetake N, Tozawa Y and Otani T 1983 *Int. J. Mech. Sci.* **25** 337-345
- [5] Da Costa Viana C S, Davies G J and Kallend J S 1978 *Textures of Materials. Proc. ICOTOM 5 2* (Germany: Springer) p 447
- [6] Pochinetto A, Pernot M and Penelle R 1981 *Deformation of Polycrystals* (Denmark: Riso National Laboratory) p 205
- [7] Rodrigues P M B and Bate P S 1985 *Texture in Non-Ferrous Metals and Alloys* AIME Warrendale PA p 173
- [8] Van Houtte P, Cauwenberg G and Aernoudt E 1987 *Mat. Sci. Eng.* **95** 115-124
- [9] Aretz H, Aegerter J and Engler O 2010 *Proc. NUMIFORM* American Institute of Physics **1252** 417-424
- [10] Engler O and Kalz S 2004 *Mat. Sci. Eng. A* **373** 350-362
- [11] Engler O and Hirsch J 2007 *Mat. Sci. Eng. A* **452-453** 640-651
- [12] Kocks U F, Tomé C N and Wenk H-R 1998 *Texture and Anisotropy* (UK: Cambridge University Press)
- [13] Engler O and Randle V 2010 *Introduction to Texture Analysis* Second Edition (USA: CRC Press)
- [14] Baldwin W M, Howald T S and Ross A W 1945 *Met. Tech. Tech. Pub.* **1808** p 86
- [15] Roberts W T 1966 *Texture Control in Sheet Metal Ind.* **43** p 237
- [16] Hug H 1965 *Aluminium und Aluminiumlegierungen* (Germany: Springer) p 412
- [17] Blade J C and Morris P L 1975 *Texture and the Properties of Materials Proc ICOTOM 4* (UK: Metals Society, Cambridge) p 171
- [18] Sheppard T and Zaidi M A 1982 *Met. Tech* **9** p 368
- [19] Kao P-W 1985 *Mat. Sci. Eng.* **74** p 147
- [20] Ma Q, Mao W, Feng H and Yu Y 2006 *Script. Mat.* **54** 1901-1905